

#### Article Info

Received : 2022-06-22 Accepted : 2022-08-19  
Revised : 2022-08-17 Available online : 2022-08-31

## Analysis of Mechanical Properties of CD 304 SS at High-Temperature Transient Conditions

Fauzi Ibrahim<sup>\*</sup>, Adi Prastyo

Mechanical Engineering Department, Engineering Faculty, Universitas Malahayati, Bandar Lampung, 35152, Indonesia

\*Corresponding Author: [fauzi@malahayati.ac.id](mailto:fauzi@malahayati.ac.id)

### Abstract

The mechanical properties of stainless steel at high temperatures are important parameters of the refractory design of stainless-steel structures. In this study, the mechanical properties of SS304 cold-drawn austenitic stainless grade at high temperature and room temperature were investigated experimentally. Thermal strain testing and total deformation of temperature transient conditions were carried out. The young modulus of maximum tensile is determined and the yield strength is determined using the 0.2% offset method. Temperature variables in this test are 25 °C, 100 °C, 200 °C, 300 °C, 400 °C, 500 °C, 600 °C, 700 °C, 800 °C, and 900 °C. In the thermal tensile test results, the specimen at 25 °C has the highest ultimate voltage ( $\sigma_u$ ), which is 698.33 MPa. Effect of temperature on the strength of SS304 stainless grade dramatically in the temperature range  $>700$  °C. High temperatures reduce steel properties to a relatively greater degree, resulting in a decrease in the mechanical properties of stainless steel SS304 grade followed by relatively low steel ductility capabilities. SEM results explain that the formation of  $\epsilon$ -martensite resulting from cold plastic deformation can lead to failure of the material at the total deformation of transient temperatures at low temperatures. The high chromium (Cr) content (~18% wt) in grade CD 304 SS can be the main trigger for the formation of Cr-carbide precipitates formed in austenite grains or grain boundaries.

### Keywords:

CD304SS, mechanical strength, transient deformation, high temperature, dislocation.

## 1 Introduction

Currently, infrastructure development in the industrial sector has increased significantly as the government's efforts to improve the economy and people's prosperity. Therefore, the need for steel for application to the main components in energy generation systems and other supporting components is also increasing, one of which is stainless steel.

Stainless steel (SS) is an alloy steel containing a minimum of 11.5% wt. Cr to increase oxidation resistance (rust resistance), especially for applications at high temperatures of 750 °C. The ability to resist rust is obtained through the formation of a layer of chromium oxide ( $\text{Cr}_2\text{O}_3$ ) which inhibits the oxidation of iron on the steel surface during application. In addition, stainless steel is used for materials with attractive appearance, corrosion resistance, low maintenance and high strength[1].

Just like steel, stainless steel also has various types indicated by the code, such as stainless steel 304 (SS304). In this study, we used an SS304 cylindrical rod shape which was produced by cold

drawing. Stainless steel 304 is austenitic type steel that has a chrome composition between 16–26% and contains at least 8% nickel, a mixture of the two elements. This will produce an austenitic layer at room temperature[2].

Regarding the performance of authentic stainless steel at high temperatures, several previous researchers have conducted research, for example [3] conducted an experimental investigation of S30408 austenitic stainless-steel material at a temperature of 200-900°C, which reported that to obtain the tensile strength of stainless steel at a temperature of low (100-300°C) in the transient state test, a tensile test of a specimen with a higher level of stress control is required. However, for a specimen with a higher level of stress control, at the beginning of the transient state test, stainless steel will quickly deform the plastic is large and at temperatures above 300°C, the deformation due to creep is more dominant, making it difficult to perform a tensile test. Therefore, at present, the lack of studies on CD 304 SS under high-temperature transient conditions is a major problem topic.

The mechanical properties of stainless steel at high temperatures are an important parameter of the fire resistance design of stainless-steel structures. However, compared to carbon steel, stainless steel has a stronger non-linear stress-strain curve, lower proportional limit, significant strain hardening, and higher strain elongation. There is a significant difference in mechanical properties between the two materials in the room and increased temperature. Thus, it is necessary to conduct more studies on the mechanical properties of stainless steel at high temperatures.

The method of design and analysis of building structures under normal conditions or room temperature has become mandatory for engineers. However, due to the frequent occurrence of building fires, the safety of the structure in a fire condition is facing an unprecedented problem and must be anticipated in its design.

There are two main test methods to find out the mechanical properties of stainless steel at high temperatures, namely the steady state test and the transient state test. In the steady state test, the specimen is first loaded to a certain pressure level and then heated according to a certain heating mode until the specimen breaks. This test method has higher requirements for testing equipment and requires a large number of specimens. However, the test conditions are closer to the actual fire location, and the results obtained by testing the interim conditions are more real, while the transient test the specimen is given a tensile load to a certain level, and the load is kept constant, then the specimen is heated to a certain temperature until plastic deformation due to temperature causes the specimen to fracture.

## 2 Materials and Methods

### 2.1 Stainless Steel 304

Stainless Steel 304 is included in the category of austenitic stainless-steel steel which contains 18% chromium and 8% nickel with the highest carbon content of 0.08%. The nickel element contained in this type of steel has an austenitic structure so that it will increase the ductility and reduce the corrosion rate. Meanwhile, the presence of carbon elements can increase the mechanical strength. Stainless Steel 304 contains a fairly low carbon maximum of 0.08%, this aims to reduce resistance to grain boundary corrosion. The chemical composition of CD 304 SS is 0.042% C, 1.19% Mn, 0.034% P, 0.006% S, 0.049% Si, 18.24% Cr, 8.15% Ni and the rest is Fe[4]. The material used in this research is stainless steel 304 in the form of a cylinder. The specimen used is a tensile test specimen based on the ASTM E 8 standard.

The material used is Stainless Steel 304 in the form of a cylinder with a diameter of 10 mm. In the manufacture of specimens on Stainless Steel 304 material is divided into 2 forms tensile testing and transient testing.

1. Tensile test specimen

In specimens for tensile testing, specimens with initial dimensions will be cut with dimensions of length and width of 220 mm x 22 mm which are then subjected to pre-strain testing.

## 2. Transient test specimen

In the transient test specimen, the specimen with the initial dimensions will be cut with the dimensions of length and width of 220 mm x 22 mm which is then carried out for transient testing.

## 2.2 Testing Method

### 1. Transient Heat Treatment

The transient heat treatment was carried out by loading the steel at a constant load rate of 3 kN/min to the desired stress level (stress levels 50, 100, 150, 200, 250, 300, 350, 400, 500 and 520MPa.). When the steel is at a stress level, then turn on the heater slowly. The temperature increase is controlled at a constant heating rate of 10°C/min to the desired temperature. This test using a temperature of 25, 100, 200, 300, 400, 500, 600, 700, 800 and 900°C. The total number of specimens for the transient condition experiment was 10 specimens. Processing of transient temperature test results data is by using the offset method.

### 2. Thermal Strain Test

In a thermal strain test, each specimen is clamped under zero load conditions, and an extensometer is attached to the measuring region of the specimen. During the thermal strain test, the axial force is maintained under zero load conditions, and the actuator is allowed to undergo axial displacement. The temperature increase in the furnace is controlled by a constant heating rate of 10°C/min until the specimen temperature is 900°C. All experimental tests, thermal strain tests, and transients were run using a personal computer with different test templates in the MTS Multipurpose Elite (MPE) software. Recording during data acquisition (DAQ), which consists of measuring specimen temperature, axial strain, axial force, displacement, and run time at a sampling frequency of 10 Hz, using MPE MTS software.

## 3 Results and Discussion.

### 3.1 Stress-Strain Curve Relationship at Room Temperature

Fig. 1 shows the strength and modulus of elasticity of austenitic stainless-steel decreases with increasing temperature. At temperatures of 800°C and 900°C the material strain gradually decreases with increasing material stress.

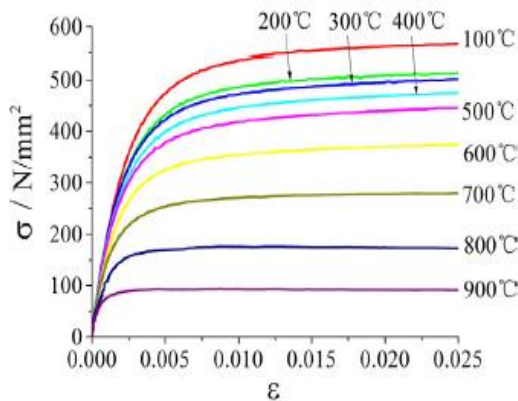


**Fig. 1.** The stress-strain curve in the tensile test of the Steady State condition of Austenitic Stainless Steel is cylindrical

Characteristics of curve voltage versus the austenitic strain of stainless-steel grade 304 manufactured under cold tensile conditions (CD304SS) are shown in Fig. 2. Typical plastic strain characteristics produced after cold drawing are generally the same

as those for steel rolling under cold working conditions[5]. Changes in properties due to plastic deformation as a manifestation of increasing steel strength through cold tensile manufacturing processes contribute to changes in plastic properties that can be observed in the plastic strain zone area. The same behavior is shown by cold-tensile low-carbon steel (CDS 1018)[6]. In contrast to the elastic zone region (Fig. 2 (Fig. inside)), nonlinear behavior can be observed in CD304SS after the stress on the material is about 400 MPa. The strain region ranges above the 0 strain offsets point. 002 mm/mm to 0.013 mm/mm, the material shows perfectly non-linear elastic behavior. This can be the cause of the initial plastic deformation trajectory at the stress level applied to the material (Fig. 2 (Fig. inside) slightly deviates from the CD304SS characteristic curve.

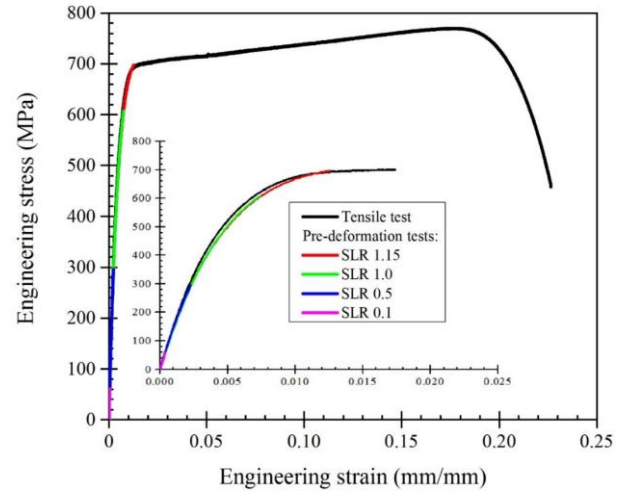


**Fig. 2.** Stress-strain characteristic curves CD304SS at room temperature conditions and initial plastic deformation characteristics at conditions below and above the yield stress of the material.

The mechanical properties of CD304SS data obtained after the static tensile test were three specimens and their average values as shown in table 1

**Table 1.** Mechanical Properties CD304SS

Specimen	Elastic modulus	Mechanical strength		Elongation
	(GPa)	(MPa)	(MPa)	(%)
	$E$	$s_y$	$s_u$	$e$
Average	153.969	607.246	775.367	49.473
STDEV	1.070	1.676	18.288	1.730

### 3.2 Thermal Strain and Coefficient of Expansion

The average thermal strain values of the three CD304SS specimens are shown in Table 2. The relationship of CD304SS axial thermal strain to temperature increase is shown in Fig. 3 which shows non-linear behavior in the direction of axial strain.

**Table 2.** Axial Thermal Strain CD304SS

Temperature (°C)	$e_{th}$ ( $\cdot 10^{-3}$ mm/mm)	STDEV ( $\cdot 10^{-4}$ )
	Average	
25	0.025	0.275
100	0.744	0.956
200	1.973	1.394
300	3.533	0.957
400	5.419	2.260
500	7.405	2.814
600	9.542	2.250
700	12.135	2.933
800	15.038	3.405
900	18.300	0.248
1000	21.274	2.896

To demonstrate the influence of manufacturing conditions and chemical composition in steel, the comparison of the axial thermal strain data of CD304SS was compared with the thermal strain value data for low carbon steel [7], [8] and the predicted model data from the Eurocode design standard for austenitic steel 304 (304SS) (EN1993,2005) and mild steel (EC3, 2012) under normal conditions. The prediction model data from Eurocode do not apply to accurately predict the thermal strain of carbon steel under cold-drawn conditions. The same can be observed in Fig. 3, a standard design for predicting the change in axial strain due to temperature for austenitic stainless steels.

A larger difference was observed in the thermal strain of CD304SS at a transient temperature of 400°C, and then the thermal strain increased significantly above the temperature of 750°C, which can generally be attributed to the phase transformation and early formation of metal-carbide precipitation through absorption of a large amount of heat[9].

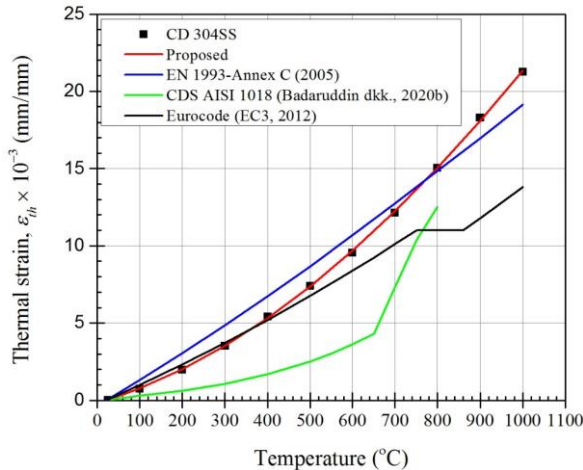


**Fig. 3.** Characteristics of the relationship of thermal strain to temperature in stainless steel and ordinary carbon steel cold drawn and normal tensile conditions

Compared to the data for ordinary carbon steel, the thermal strain value of CD304SS is higher. Therefore, by observing the axial thermal strain data shown in Fig. 3, it is very clear that the manufacturing process and chemical composition in steel affect the axial thermal strain behavior. This statement was also made clear by [10] in investigating low carbon steel (S355J2) under hot rolling conditions lower than predicted by the EC3 thermal strain data model at temperatures above up to 900°C. In addition, the thermal strain trend for high strength steel (HSS) grade S690QL and high strength steel above 900 MPa (S960QL) under quenching and tempering (Q&T) manufacturing conditions showed almost the same behavior at temperatures up to 600 °C[11].

As compared to the data shown in Fig. 3 and the findings of several previous researchers, the cold drawing process and the chemical composition in the steel significantly affect the axial thermal strain behavior of CD304SS. Therefore, we propose a model for predicting the axial thermal strain of cold tensile stainless steel 304 (CD304SS) in the form of an equation of the thermal strain-temperature relationship that expresses a temperature function in the temperature range of 25-1000°C. The prediction equation for this model is expressed in the form of a quadratic polynomial equation using the square curve fitting method with a rational value of R squared (R<sup>2</sup>) 99% in the form of an Eq. (1):

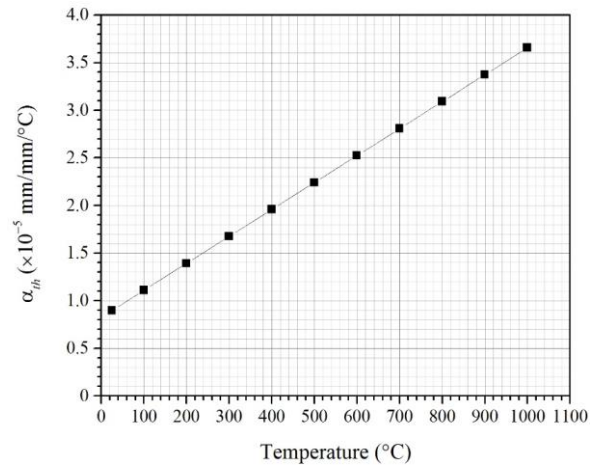
$$\epsilon_{th} = 1.288 \times 10^{-5} T^2 + 8.766 \times 10^{-3} T - 2.408 \times 10^{-1} \quad (1) \quad (25^\circ\text{C} \ll T \ll 1000^\circ\text{C})$$

The coefficient of thermal expansion of CD304SS is obtained by differentiating Eq. (1) concerning temperature (T), which

describes the change in axial deformation in units of mm/mm and per degree Celsius, (Eq. 2):

$$\alpha_T = \frac{d\epsilon_{th}}{dT} = 2.576 \times 10^{-5} T + 8.766 \times 10^{-3} \quad (25^\circ\text{C} \ll T \ll 1000^\circ\text{C}) \quad (2)$$

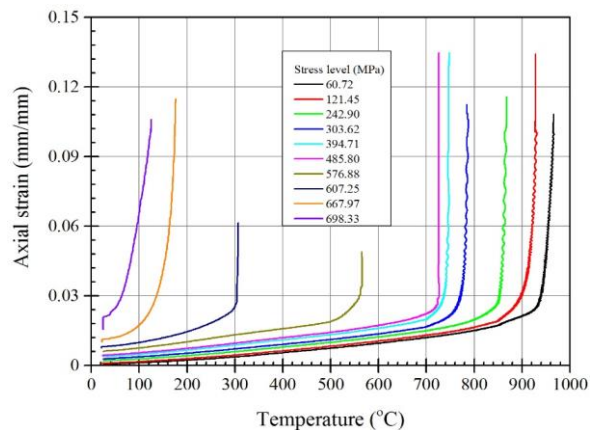
Equality indicates (2) substantially that thermal expansion CD304SS depicts linear behavior concerning temperature (Fig. 4). Therefore, the slope of the linear thermal expansion curve shown in Fig. 4 indicates austenitic stainless-steel grade 304 SS manufactured under cold-drawing conditions resulting in a constant coefficient of thermal expansion of  $2.576 \times 10^{-5}$  mm/mm/°C.



**Fig. 4.** The plot of the thermal expansion numerical data for CD304SS obtained from Eq. (2) to temperature

### 3.3 Effect of Transient Temperature on Mechanical Properties

Fig. 5 displays the characteristics of a typical CD304SS temperature-strain relationship curve after a total deformation test with transient temperature. The failure temperature experienced by the material during transient temperature deformation shows a dependence on the stress level applied to produce the initial plastic deformation.



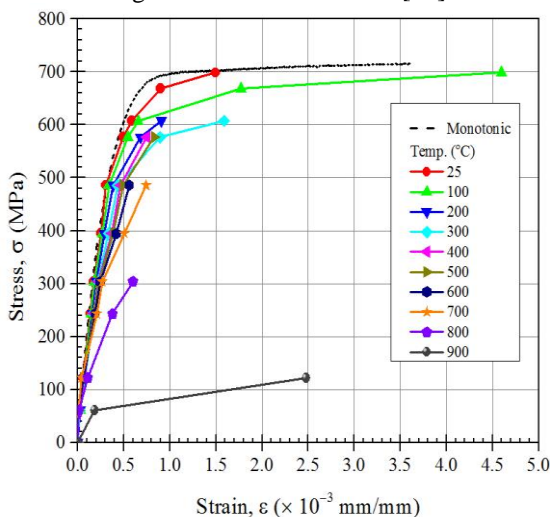
**Fig. 5.** CD304SS temperature-strain relationship on the initial plastic deformation rate due to different stresses

Fig. 5 shows that there are three zones where the effect of transient temperature on the magnitude or degree of initial plastic deformation in a given CD304SS is shown. The first zone is categorized as the temperature at which CD304SS fails due to transient temperatures below 200°C (categorized as the low-temperature zone). The second zone is the zone where CD304SS fails in the temperature range of 300°C to 700°C (high-temperature zone). While the third zone where the failure of CD304SS is in the range of transient temperature >700°C and

~1000°C (supercritical temperature). The failure temperature of CD304SS from the stress level of 668 MPa (1.1 $\sigma_y$ ) to the highest stress level of 698 MPa (~1.15 $\sigma_y$ ) (Fig. 5) indicates the failure of CD304 at relatively low-temperature conditions. This effect is mainly due to the low plastic deformation ability of the material due to the excessive plastic deformation effect. The initial deformation given to CD304SS in the range of stress levels in the proportional limit region of the yield strength of the material (~0.8 $\sigma_y$ ) indicates the failure of the material at a transient temperature of >700°C.

This phenomenon can be attributed to the relatively large plastic deformation capacity of CD304SS. This explanation is confirmed by the characteristics of the stress-strain curve shown in Fig. 2. Generally, the steel manufacturing process through cold drawing causes the grain structure of the material to undergo a longitudinal change in shape following the direction of steel pulling which causes an increase in the high dislocation density and causes the material to become strong[12]. This amplification mechanism can be attributed to a decrease in the distance between the phases in the area around the grain boundaries, which effectively allows the dislocation motion to be hindered, leading to an increase in the high dislocation density. In addition, the distortion of the atoms in the austenite matrix triggers the carbon atoms to form martensite (lath  $\epsilon$ -martensite)[13], [14]. Therefore, hardening through the dislocation-strain coupling mechanism results in a large residual compressive stress in the axial direction [15], [16] and the formation of  $\epsilon$ -martensite solid solution particles is the main source of increasing the mechanical strength of 304SS under cold tensile conditions. Thus, the mechanical strength of CD304SS is significantly increased. In contrast, CD304SS has a low capacity for subsequent plastic deformation during tensile deformation at room temperature. Therefore, we conclude that when CD304SS under cold-drawn conditions is loaded until nominal yield strength is reached, CD304SS becomes susceptible to thermal deformation with increasing temperature (Fig. 5).

Under transient conditions, the mechanical properties of CD304SS were obtained using a procedure similar to that used by [17] whose procedure was described in methods. A typical CD304SS stress-strain curve obtained experimentally through a series of axial thermal strain tests (Fig. 3) and the total deformation temperature transient (Fig. 5) is shown in Fig. 6. Observations on the elastic region of the stress-strain curve in Fig. 6 show the strain in the elastic section, slightly shows nonlinear behavior. These changes are generally experienced by steel as a result of the combination of materials experiencing elongation due to thermal strain and constant stress (creeping due to creep)[18]. Therefore, the modulus of elasticity of CD304SS was determined conventionally using the tangent modulus recommended by ASTM in standard E111 (2004), and the yield strength was determined using the 0.2% offset method[19].



**Fig. 6.** Characteristics of the stress-strain curve obtained from transient temperature deformation and static (monotonic) tensile test

The mechanical properties of CD304SS which consist of elastic modulus (E), yield strength ( $\sigma_y$ ), and maximum strength ( $\sigma_u$ ) were derived from the transient method at room temperature plastic deformation (25°C) and high temperature transient conditions (ET, y, T, and u, T) are presented in table 3.

**Table 3.** Mechanical properties of CD304SS at different temperatures obtained using the transient method

Temp. (°C)	Mechanical Strength (MPa)		Young Modulus (GPa) E	Factor Reduction		
	$S_y$	$S_{ult}$		$S_{y, T}/S_y$	$S_{ult, T}/S_{ult}$	$E_T/E$
25	579.702	698.333	195.954	1.000	1.000	1.000
100	572.238	698.333	193.472	0.987	1.000	0.987
200	517.837	607.246	186.973	0.893	0.870	0.954
300	397.458	607.246	186.278	0.686	0.870	0.951
400	327.779	576.884	191.542	0.565	0.826	0.977
500	311.226	576.884	135.139	0.537	0.826	0.690
600	292.822	485.797	127.897	0.505	0.696	0.653
700	319.978	485.797	94.528	0.552	0.696	0.482
800	259.945	303.623	57.741	0.448	0.435	0.295
900	82.577	121.449	28.951	0.142	0.174	0.148

Also, the ratio of the decrease in mechanical strength due to temperature is expressed by a reduction factor as a result of the comparison of the value of the mechanical strength at the transient temperature with the mechanical properties obtained at a temperature of 25°C (Table 3).

Fig. 7 and 8 demonstrate the dependence of mechanical strength and elastic modulus, respectively, under transient high-temperature conditions for CD304SS. The effect of temperature on the strength of CD304SS is dramatic in the temperature range >700°C. High temperatures degrade the steel properties to a relatively large extent, resulting in a decrease in the mechanical properties of CD304SS steel followed by a relatively low ductility of the steel. Under these conditions, the mechanical property dependence was associated with a similar effect to that of cold-tensile AISI 1018 steel[7]. Whereas temperature dependence on temperature range >300°C to 700°C, may be due to the blue brittleness phenomenon[9].

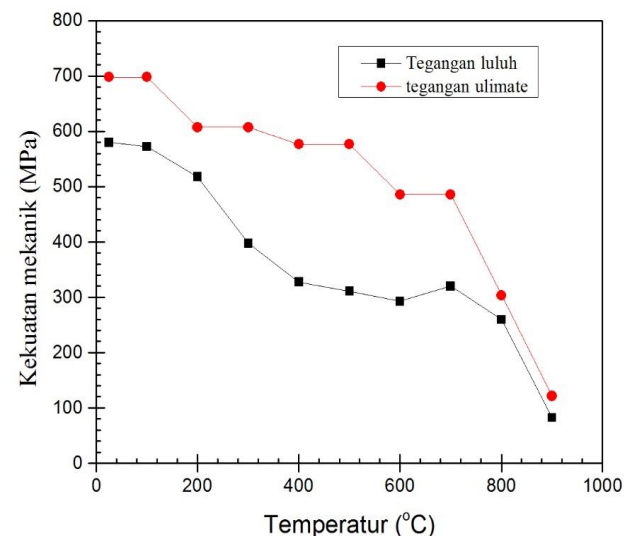


**Fig. 7.** The dependence of the tensile strength of CD304SS on the temperature of the transient condition

Meanwhile, at a temperature of up to 400°C, the elastic modulus of the material decreases slowly, dropping drastically linearly to a temperature of 900°C (Fig. 8). This finding is somewhat similar to that reported by [20] where temperatures ranging from 425 to 475°C entering the cold drawn high carbon steel wire triggers the diffusion of dissolved carbon atoms from

cementite carbide into the grain boundaries and causes grain boundary distortion.

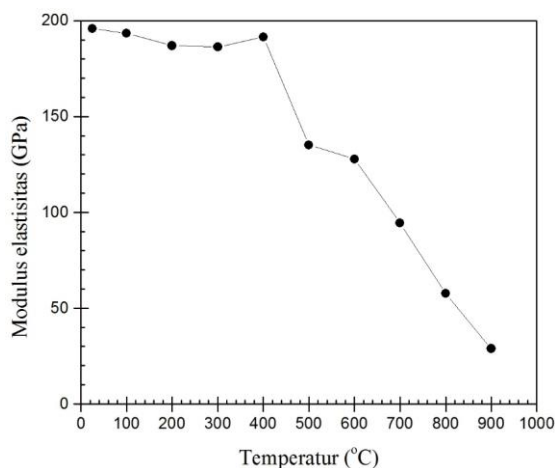


**Fig. 8.** The dependence of the elastic modulus of CD304SS on the temperature of the transient condition.

Furthermore, [10], [11] confirmed the degradation of the mechanical properties of S355 hot-rolled steel under normal conditions at 400°C could be attributed to the high Mn content in the steel which could trigger the formation of manganese-sulfide (Mn-S). This explanation is supported by the finding [21] that the content of 1, The higher 0% by weight of Mn in high-strength steels could be the cause of the tensile anisotropy due to the formation of elongated Mn-sulphide (MnS) inclusions during tensile deformation. It is interesting from the results of this study, that the formation of  $\epsilon$ -martensite resulting from cold plastic deformation can trigger material failure at transient temperatures and total deformation at low temperatures (Fig. 5). It has been described in detail the process of forming martensite on austenitic steel 304 produced through a cold deformation process [13], [14]. The extremely low ability of martensite in low-alloy steels to subsequent plastic deformation triggers the softening behavior of the steels as has been reported by [7]–[9]. The hardening effect of AISI 4140 alloy steel produced by Q&T has a detrimental effect on the cyclic plastic deformation ability. Due to the effect of martensite in steel at high temperatures, martensite is a metastable phase in which carbon atoms readily diffuse out towards the grain boundaries to form metal-carbides as precipitation or inclusion of particles in the steel microstructure, depending on the type of metal elements that become alloys in the steel. In this study, the high chromium (Cr) content (~18% wt.) in cold-tensioned grade 304 stainless steel could be the main trigger for the formation of Cr-carbide precipitation that forms in austenite grains or grain boundaries. This precipitation will increase in size with increasing temperature, the presence of which in the austenite matrix decreases the mechanical strength of the steel when the steel is exposed to relatively high temperatures [11], [22].

### 3.4 Fractographic analysis and failure types

Fig. 9 reveals the morphology of typical fracture surfaces of the CD304SS specimen at low (left) and high (right) magnifications after transient temperature total plastic deformation testing and static tensile testing. The increase in initial plastic deformation is accompanied by a lower strain hardening capacity, but the fault features produce ductile fracture characteristics indicated by the number of dimple fractures (Fig. 9(b) and (c)). Generated by the nucleation, growth, and fusion of micro voids during the phenomenon of axial plastic deformation due to temperature. In addition, it was also observed in the fracture pattern of the indentation for the samples tested under static tension conditions at room temperature (Fig. 9(d)).

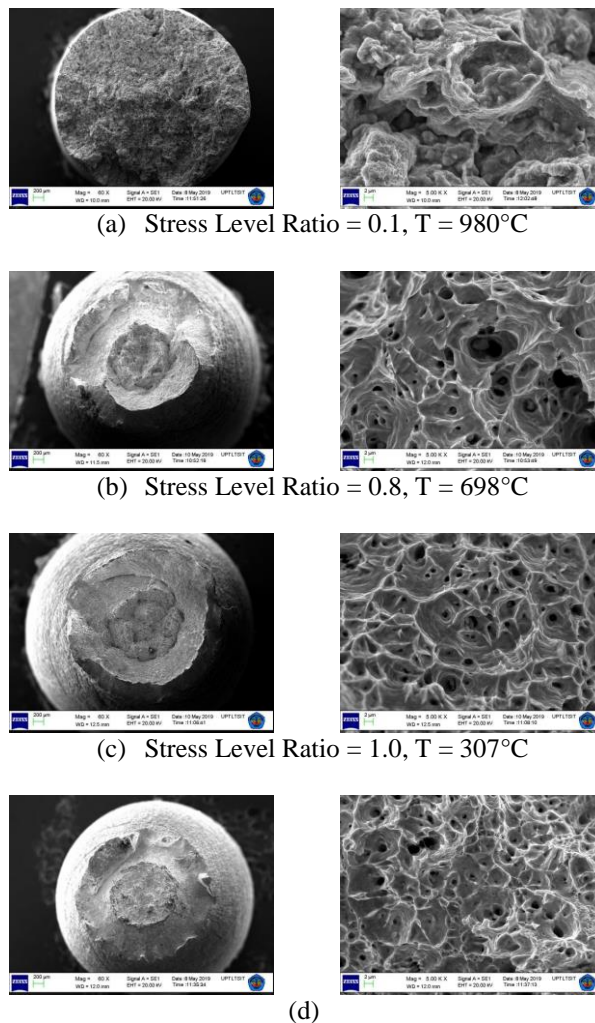


**Fig. 9.** (a-c) SEM fractography of the surface fracture of CD304SS at different ratios of stress and temperature levels (T) and (d) SEM of fracture of the surface of the sample from the static tensile test at room temperature

Meanwhile, indentation fractures with a relatively small number of indentations were found in the CD304SS sample which was tested for total transient temperature deformation at a stress level of  $0.1\sigma_y$  (Fig. 9(a)). This observation was also clarified from the results of the fracture type of the specimen at the stress ratio condition of  $0.1\sigma_y$  shown in Fig. 10. The number of indentations resulting from the fracture shown in Fig. 9.a and the type of fracture of the specimen in Fig. 10 indicate a brittle fracture.



**Fig. 10.** CD304SS failure type under transient temperature total deformation condition

The significant difference between ductile and brittle fracture can be explained as follows: The fracture morphology of the sample in Fig. 9(b) and (c) clearly shows many indentations with several smaller voids within the grain and several larger voids on the fracture surface of the specimen. While the brittle fracture model can be related to the formation of voids resulting from the diffusion process of carbon or chromium atoms and where the voids core and grow in regions consisting of high-stress concentrations in austenite/martensite or martensite/precipitation matrices [14] which contain a lot of sediment. carbide with high strain energy[23].

These voids continue to expand with increasing transient temperature reaching a critical temperature of  $\sim 900^{\circ}\text{C}$  and coalesce with each other as plastic deformation increases due to temperature (axial thermal strain).

The combination produced by the magnitude of thermal strain and creep due to constant stresses cause the material to fail in a brittle state. As for the materials with the ability, the low plastic deformation due to the large initial deformation ( $1.0 \sigma_y$ ) resulted in a ductile fracture (Fig. 9(c)). The fractography of the sample shown in Fig. 9.c shows fractographic features that are relatively similar to the sample tested for tensile strength under RT conditions (Fig. 9(d)). The significant difference in the fracture surface of the samples tested at RT and the fracture surface of the samples subjected to a higher failure temperature of  $700^{\circ}\text{C}$  can be attributed to the increase in indentation size with increasing transient temperature. The increase in the dimple size of the fracture surface SEM observations in Fig. 9(a), under low and high magnification, displays the coarse microstructure that occurs during temperature deformation, indicating that recovery and recrystallization have begun. This observation is similar to the observed fracture surface of VHS-31.8 steel pipe under quenching conditions at temperatures ranging from  $100^{\circ}\text{C}$  to  $600^{\circ}\text{C}$ [24]. The indentations formed on the steel surface are relatively rough and few can be attributed to the formation of chromium-carbide precipitation which increases with increasing temperature. At higher transient temperatures experienced steel with a deformation stress level of  $0.1 \sigma_y$ , indicating that the recovery and crystallization process may have started at temperatures  $>700^{\circ}\text{C}$  (Fig.3) followed by a drastic reduction in the mechanical properties of CD304SS (Table 3) and demonstrated in Fig. 7. Under these conditions, the microstructure which has decreased distortion energy becomes a reservoir for carbon and chromium atoms to diffuse to form Cr-carbide precipitation which is detrimental[24]. During the diffusion of dissolved carbon atoms in the martensite or matrix (austenite), A typical failure type of CD304SS tensile specimen under transient conditions at different stress levels is shown in Fig. 9. All steel specimens experienced a tensile failure resulting in a reduction in the cross-sectional area of the fracture (necking), which indicates a relatively ductile CD304SS failure. Steel specimens experienced the highest ductile fracture ( $\sim 60\%$  area reduction) at stress levels of  $0.2\text{--}0.8 \sigma_y$  wherein the specimens failed at  $700^{\circ}\text{C}$ . However, different fracture patterns were found in the steel samples subjected to  $0.1 \sigma_y$  load, where the steel specimens failed above  $950^{\circ}\text{C}$ . In addition, the reduction of the fracture cross-section (Fig. 10) is relatively lower compared to some other specimens at the level. ratio different voltage. This phenomenon can be attributed to the phase transformation and formation of Cr-carbide which triggers distortion in the steel due to limited plastic deformation ability and eventually leads to brittle failure.

#### 4 Conclusions.

In the CD304SS tensile test results, the strain and stress value curves are obtained, the stress value obtained from the CD304SS tensile test results is 400 (MPa) while the strain value obtained from the CD304SS tensile test is 0.002 mm/mm to 0.013 mm/mm,

can cause path deformation initial plasticity at the stress level applied to the material. In the results of the thermal tensile test, the increasing temperature used will decrease the ultimate stress value (MPa) and will decrease the value of the elastic modulus (GPa), to determine the change in axial strain due to the austenitic stainless-steel temperature, indicating that the thermal strain of CD304SS is in the temperature range of 25 temperature  $750^{\circ}\text{C}$  shows a linear behavior concerning temperature, thus showing the slope of the linear thermal expansion curve. The increase in temperature causes CD304SS to be susceptible to thermal deformation, this is indicated by the failure of the material at transient temperatures  $>700^{\circ}\text{C}$ . The effect of temperature on the strength of CD304SS dramatically in the temperature range  $>700^{\circ}\text{C}$  which results in a decrease in the mechanical properties of CD304SS steel followed by a relatively low ductility of steel with an elastic modulus value of only 100 GPa. SEM results explain that the formation of  $\epsilon$ -martensite resulting from cold plastic deformation can trigger material failure at transient temperatures and total deformation at low temperatures. A typical type of failure of the CD304SS tensile specimen under transient conditions at different stress levels shows that all steel specimens experience tensile failure resulting in a reduction in the cross-section of the fracture area (necking), which indicates a relatively ductile failure of CD304SS. Steel specimens experienced the highest ductile fracture (area reduction  $\sim 60\%$ ) at stress levels of  $0.2\text{--}0.8 \sigma_y$  wherein the specimens failed at  $700^{\circ}\text{C}$ .

#### References

- [1] J. G. Thakare, C. Pandey, M. M. Mahapatra, and R. S. Mulik, "An assessment for mechanical and microstructure behavior of dissimilar material welded joint between nuclear grade martensitic P91 and austenitic SS304 L steel," *J. Manuf. Process.*, vol. 48, pp. 249–259, 2019.
- [2] T. Jiang, L. Peng, P. Yi, and X. Lai, "Analysis of the electric and thermal effects on mechanical behavior of SS304 subjected to electrically assisted forming process," *J. Manuf. Sci. Eng.*, vol. 138, no. 6, 2016.
- [3] S. Fan, L. Jia, X. Lyu, W. Sun, M. Chen, and J. Zheng, "Experimental investigation of austenitic stainless steel material at elevated temperatures," *Constr. Build. Mater.*, vol. 155, pp. 267–285, 2017.
- [4] R. Joham, N. K. Sharma, K. Mondal, and S. Shekhar, "Low temperature cross-rolling to modify grain boundary character distribution and its effect on sensitization of SS304," *J. Mater. Process. Technol.*, vol. 240, pp. 324–331, 2017.
- [5] H. Fang, T.-M. Chan, and B. Young, "Material properties and residual stresses of octagonal high strength steel hollow sections," *J. Constr. Steel Res.*, vol. 148, pp. 479–490, 2018.
- [6] M. Badaruddin, H. Wardono, H. Supriadi, and M. Salimor, "Experimental investigation of mechanical properties of cold-drawn AISI 1018 steel at high-temperature steady-state conditions," *J. Mater. Res. Technol.*, vol. 9, no. 2, pp. 1893–1904, 2020.
- [7] M. Badaruddin, A. Sugiri, and C. J. Wang, "An experimental investigation of the mechanical strength of cold-drawn AISI 1018 steel under high-temperature steady-and transient-state conditions," *Constr. Build. Mater.*, vol. 232, p. 117193, 2020.
- [8] M. Badaruddin, H. Wardono, C. J. Wang, and A. K. Rivai, "Improvement of low-cycle fatigue resistance in AISI 4140 steel by annealing treatment," *Int. J. Fatigue*, vol. 125, pp. 406–417, 2019.
- [9] Y. Du, J. Peng, J. Y. R. Liew, and G. Li, "Mechanical properties of high tensile steel cables at elevated temperatures," *Constr. Build. Mater.*, vol. 182, pp. 52–65, 2018.

- [10] M. Neuenschwander, M. Knobloch, and M. Fontana, "Elevated temperature mechanical properties of solid section structural steel," *Constr. Build. Mater.*, vol. 149, pp. 186–201, 2017.
- [11] M. Neuenschwander, C. Scandella, M. Knobloch, and M. Fontana, "Modeling elevated-temperature mechanical behavior of high and ultra-high strength steels in structural fire design," *Mater. Des.*, vol. 136, pp. 81–102, 2017.
- [12] Z. Tao, "Mechanical properties of prestressing steel after fire exposure," *Mater. Struct.*, vol. 48, no. 9, pp. 3037–3047, 2015.
- [13] D. Xu, X. Wan, J. Yu, G. Xu, and G. Li, "Effect of cold deformation on microstructures and mechanical properties of austenitic stainless steel," *Metals (Basel)*, vol. 8, no. 7, p. 522, 2018.
- [14] S. K. Ghosh, P. Mallick, and P. P. Chattopadhyay, "Effect of cold deformation on phase evolution and mechanical properties in an austenitic stainless steel for structural and safety applications," *J. Iron Steel Res. Int.*, vol. 19, no. 4, pp. 63–68, 2012.
- [15] S. Sato *et al.*, "Relationship between dislocations and residual stresses in cold-drawn pearlitic steel analyzed by energy-dispersive X-ray diffraction," *Mater. Charact.*, vol. 83, pp. 152–160, 2013.
- [16] L. Zhou, F. Fang, L. Wang, H. Chen, Z. Xie, and J. Jiang, "Torsion delamination and recrystallized cementite of heavy drawing pearlitic wires after low temperature annealing," *Mater. Sci. Eng. A*, vol. 713, pp. 52–60, 2018.
- [17] X. Qiang, F. Bijlaard, and H. Kolstein, "Dependence of mechanical properties of high strength steel S690 on elevated temperatures," *Constr. Build. Mater.*, vol. 30, pp. 73–79, 2012.
- [18] G. Yuan, Q. Shu, Z. Huang, and Q. Li, "An experimental investigation of properties of Q345 steel pipe at elevated temperatures," *J. Constr. Steel Res.*, vol. 118, pp. 41–48, 2016.
- [19] A. Standard, "E8, Standard test method for tension testing of metallic materials, West Conshohocken (USA), ASTM," 2004.
- [20] I. Azmy, M. A. K. Umam, and R. Muliawan, "Studi pengaruh proses tempering terhadap struktur mikro dan kekerasan post-annealing baja mangan austenitik," *J. Polimesin*, vol. 19, no. 2, pp. 169–175, 2021.
- [21] F. Fakhriza, S. Huzni, M. Murtadhahadi, and A. Dabet, "Studi perbandingan perilaku lelah AISI 316L dengan menggunakan metode eksperimen dan simulasi," *J. Polimesin*, vol. 19, no. 2, pp. 194–200, 2021.
- [22] S. Hosseini, A. Heidarpour, F. Collins, and C. R. Hutchinson, "Strain ageing effect on the temperature dependent mechanical properties of partially damaged structural mild-steel induced by high strain rate loading," *Constr. Build. Mater.*, vol. 123, pp. 454–463, 2016.
- [23] M. V. Kumar, V. Balasubramanian, and A. G. Rao, "Hot tensile properties and strain hardening behaviour of Super 304HCu stainless steel," *J. Mater. Res. Technol.*, vol. 6, no. 2, pp. 116–122, 2017.
- [24] A. Heidarpour, N. S. Tofts, A. H. Korayem, X.-L. Zhao, and C. R. Hutchinson, "Mechanical properties of very high strength steel at elevated temperatures," *Fire Saf. J.*, vol. 64, pp. 27–35, 2014.